CHAPTER IV
DEM SIMULATION

Discrete numerical simulation of particles has been used in a wide range for research of physical phenomena, including galaxy formation, plasma behavior and fluid turbulence. This technique was known as Distinct or Discrete Element Method (DEM). P.A. Cundall and O.D.L. Strack (1979) proposed this method for analyzing the stability of fractured rock slopes. DEM has been used primarily to study the fabric and structure of granular media and to assist in the development of constitutive relations of soil. In recent years, DEM Simulation has been proved that it is a powerful tool in powder technology.

4.1 Distinct or discrete element method

The principle of distinct element method (DEM) is based on the nature of a fictitious material. In the DEM, the equilibrium contact forces and displacements of a stressed assembly of discs or spheres are found through a series of calculations tracing the movements of the individual particles. These movements are the result of the propagation through the medium of disturbances originating at the boundaries: a dynamic process. The speed of propagation is a function of the physical properties of the discrete medium. The DEM is based upon the idea that the time step chosen should be sufficiently small that during a single time step disturbances cannot propagate from any particle further than its immediate neighbours. At all time the resultant forces on any particle are determined exclusively by its interaction with the surrounding particles with which it is in contact.

4.1.1 Calculation cycle

The calculations in DEM rely on the application of Newton's second law to the particles and force-displacement law during the contacts. Newton's second law gives the motion of a particle resulting from the forces acting on it. The force displacement law is used to find contact forces from displacement. The deformations of the individual particles are small in comparison with deformation of a granular assembly as a whole. The latter deformation is due primarily to the

movements of the particles as rigid bodies. Therefore, precise modeling of particle deformation is not necessary to obtain a good approximation of the mechanical behavior. The particles are allowed to overlap one another at contact point in the calculation algorithm. The overlapping behavior takes place in lieu of the deformation of the individual particles. The magnitude of the overlap is considered to be related directly to the contact force. It should be noted that these overlaps are small in relation to the particle size. To illustrate how forces and displacement are determined during a calculation cycle, the case 2-dimentional represented in Figure 4.1(a) will be considered. Two weightless particles, labeled as particle x and particle y, are squashed between a pair of rigid walls. The walls move toward each other at a constant velocity v. Initially, at time $t = t_0$, the wall and discs are touching and no contact forces exist. At time Δt later, the wall has moved inward over a distance $v\,\Delta t$. In accordance with the assumption that the disturbances cannot travel beyond a single disc during one time step, both particles are assumed to maintain their initial positions during the time interval from $t = t_0$ to $t = t_0 + \Delta t$. Overlap therefore exist at time $t_1 = t_0 + \Delta t$ at contacts A and C as shown in Figure 4.1(b) and are of magnitude $\Delta n = v\,\Delta t$. Points A(D) and A(W) in Figure 4.1(b) are points of the particle and the wall, respectively, lying on the line drawn perpendicular to the wall and through the center of the particle. The contact A is defined as the point halfway between $A_{(D)}$ and $A_{(W)}$. The relative displacement $(\Delta n_{(A)})_{t1}$ at the contact (the overlap) is defined as the displacement of point $A_{(W)}$ relative to that of point $A_{(D)}$ occuring over one time increment. The subscript t_1 in $(\Delta n_{(A)})_{t1}$, refers to the time. The relative displacements occuring at contacts A and C at time $t_1 = t_0 + \Delta t$ as shown in Figure 4.1(b) are used in a force-displacement law for the calculation of contact forces. An increment force-displacement law of the following form is used

$$\Delta F_n = k_n (\Delta n)_{t1} = k_n v \Delta t \qquad (4.1)$$

Where k_n is the normal stiffness and ΔF_n represents the increment in normal force. Defining the positive 1 direction as pointing from particle x to particle y (Figure 4.1(b)) the sums of force $F(x)_1$ and $F(y)_1$ for particle x and y at time $t_1 = t_0 + \Delta t$ become, taking $F(x)_1$ and $F(y)_1$ to be position in the positive 1 direction

$$F(x)_1 = k_n (\Delta n)_{t1} \qquad F(y)_1 = - k_n (\Delta n)_{t1} \tag{4.2}$$

These forces are used to find new accelerations using Newton's second law

$$\ddot{x}_1 = \frac{F_{(x)1}}{m_{(x)}} \qquad \ddot{y}_1 = \frac{F_{(y)1}}{m_{(y)}} \tag{4.3}$$

Where $\ddot{x}_1$ and $\ddot{y}_1$ are accelerations of particle x and y in the 1 direction. The subscripts (x) and (y) in the masses $m_{(x)}$ and $m_{(y)}$ refer to particle x and y. The accelerations found from Equation (4.3) are assumed to be constant over the time interval from $t_1 = t_0 + \Delta t$ to $t_2 = t_0 + 2\Delta t$ and may be integrated to yield velocities

$$[\dot{x}_1]_{t2} = \left[\frac{F_{(x)1}}{m_{(x)}}\right]\Delta t \qquad [\dot{x}_2]_{t2} = \left[\frac{F_{(y)1}}{m_{(y)}}\right]\Delta t \tag{4.4}$$

The relative displacement increments at contacts A, B and C at time $t_2 = t_0 + 2\Delta t$ are found from

$$\left(\Delta n_{(A)}\right)_{t2} = \left(v - \left[\frac{F_{(x)1}}{m_{(x)}}\right]\Delta t\right)\Delta t \tag{4.5}$$

$$\left(\Delta n_{(B)}\right)_{t2} = \left(\left[\frac{F_{(x)1}}{m_{(x)}}\right]\Delta t - \left[\frac{F_{(y)1}}{m_{(y)}}\right]\Delta t\right)\Delta t \tag{4.6}$$

$$\left(\Delta \boldsymbol{n}_{(C)}\right)_{t2} = \left(\left[\frac{\boldsymbol{F}_{(y)1}}{m_{(y)}}\right]\Delta t - [-\boldsymbol{v}]\right)\Delta t \tag{4.7}$$

Where $\Delta n_{(A)}$, $\Delta n_{(B)}$ and $\Delta n_{(C)}$ are taken as positive for compression. This cycle may be repeated again and again: forces corresponding to the displacements are found using the force displacement law, Equation (4.2), and the force sums for the two particles are substituted in Newton's second law, Equation (4.3), to obtain displacements. In the general case of an assembly of numerous particles, the force –displacement law is applied at each contact of any disc and the vectorial sum of these contact forces is determined to yield the resultant force acting on that particle. When this has been accomplished for every particle, new accelerations are calculated from Newton's second law.

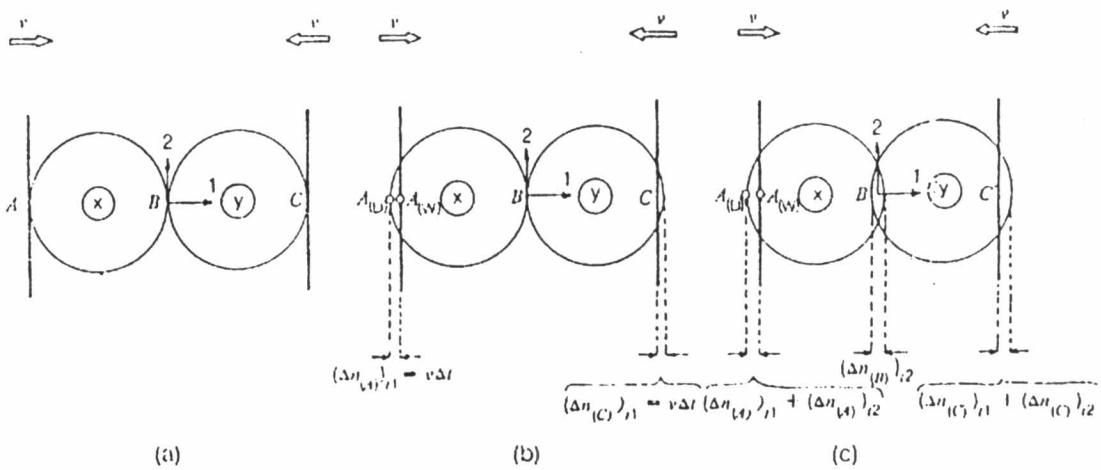

Figure 4.1 Two discs compressed between rigid walls (the overlaps are exaggerated)

(a) $t = t_0$: (b) $t = t_1 = t_0 + \Delta t$: (c) $t = t_2 + 2\Delta t$

4.2 Equations of particle and fluid motion

The basic equations for the gas and particle motion, and the general concept of the calculations are explained as follows.

4.2.1 Particle motion

Particles and quasi-static flow are in contact with the surrounding particles or the wall. Since each particle has elasticity, a particle assembly forms a complicated vibrationary system having multiple degrees of freedom. Moreover the contact points change with time. The influence of a particle on the other particles far from it propagates in a disturbance wave. It is very difficult to consider the interaction between one particle and remote ones. If the time step in numerical calculation is chosen sufficiently small, it can be assumed that during the single time step disturbances do not propagate from any particles further than its immediate neighbors. In other words, the instantaneous motion of each particle is determined by contact forces between that particle and the particle which it is in contact with. An assembly of spherical particles of uniform size is considered. Individual particles have two types of motion as follows: translational and rotational motions. Equations of translational and rotational particle motion are the following:

$$\dot{\boldsymbol{v}} = \frac{\boldsymbol{F}}{m} + \boldsymbol{g} \tag{4.8}$$

$$\dot{\boldsymbol{\omega}} = \frac{\boldsymbol{T}}{I} \tag{4.9}$$

Where $\dot{\boldsymbol{v}}$ is the particle velocity vector, m is the particle mass, F is the sum of forces acting on the particle, g is the gravity acceleration vector, $\dot{\boldsymbol{\omega}}$ is the angular velocity, T is the net torque caused by the contact force, I is the moment of inertia of the particle, and superscript (.) denotes a time derivative. The force F consists of contact forces and fluid forces. The new velocities and position after the time step Δt are given by

$$\boldsymbol{v}_s = \boldsymbol{v}_{s0} + \dot{\boldsymbol{v}}_{s0}\Delta t \tag{4.10}$$

$$\boldsymbol{r} = \boldsymbol{r}_0 + \boldsymbol{v}_s\Delta t \tag{4.11}$$

$$\omega = \omega_0 + \dot{\omega}_0 \Delta t \tag{4.12}$$

where v is the velocity vector, subscript 0 denotes the old value, and subscript s refers to the particle. The force F can be divided into the contact force and fluid force as $\boldsymbol{F} = \boldsymbol{f}_C + \boldsymbol{f}_D$

4.2.2 Modeling of contact forces

Cundall and Strack (1979) use the model shown in Figure 4.2(a) to formulate the contact forces between two spheres. The model consists of a spring, a dash-pot and a slider. The model of the contact with the wall is shown in Figure 4.2(b). The effects of these mechanical elements on particle motion appear through the following parameters: stiffness (k), damping coefficient (η) and friction coefficient (μ_f).

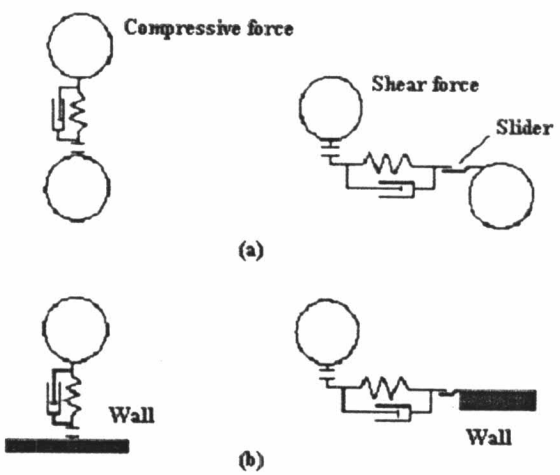

Figure 4.2 Models of contact force: (a) particle-to-particle (b) particle-to-wall

When particle i is contact with particle j, the normal component of the contact force, $\boldsymbol{f}_{Cnij}$, acting on particle i is given by the sum of the forces due to the spring and the dash-pot:

$$\boldsymbol{f}_{Cnij} = \left(-k\delta_{nij} - \eta_n \boldsymbol{v}_{rij} \cdot \boldsymbol{n}_{ij}\right)\boldsymbol{n}_{ij} \tag{4.13}$$

Where δ_{nij} is the particle displacement caused by the normal force, v_{rij} is the velocity vector of particle i relative to particle j, and n_{ij} is the unit vector from the center of particle i to that of particle j. The tangential component of the contact force, f_{Ctij} is given by

$$f_{Ctij} = -k_t \sigma_{tij} - \eta_{tj} v_{sij} \tag{4.14}$$

where k_t and σ_{tij} are the stiffness and displacement in the tangential direction respectively. The suffixes n and t are the components corresponding to the normal and tangential directions respectively. v_{sij} is the slip velocity of the contact point, which is given by

$$v_{sij} = v_{rij} - (v_{rij} \cdot n)n + r_s(\omega_i + \omega_j) \times n \tag{4.15}$$

where r_s is the radius of the sphere. When particle j is replaced by the wall, $|v_j| = |\omega_j| = 0$. If the following relation is satisfied

$$|f_{Ctij}| > \mu_f |f_{Cnij}| \tag{4.16}$$

then particle i slides and the tangential force is given by

$$f_{Ctij} = -\mu_f |f_{Cnij}| t_{ij} \tag{4.17}$$

instead of Equation (4.14) . Equation (4.17) is the Coulomb-type friction law. The displacement is given by

$$\sigma_{tij} = \left(\frac{1}{k_t}\right) f_{Ctij} \tag{4.18}$$

$\vec{t}_{ij}$ is the unit vector defined by

$$\boldsymbol{t}_{ij} = \frac{\boldsymbol{v}_{sij}}{|\boldsymbol{v}_{sij}|} \tag{4.19}$$

The damping coefficient can be determined from coefficient of restitution (e) as

$$\eta = \frac{-2\ln(e)}{\sqrt{\pi^2 + (\ln(e))^2}} \tag{4.20}$$

The same relations as the above equations are derived for contact with the wall if particle j is replaced by the wall. In general, a few particles are in contact with particle i at the same time. Therefore the total acting on particle i is obtained by taking the summation of the above forces with respect to j:

$$\boldsymbol{f}_{Ci} = \sum_j \left(\boldsymbol{f}_{Cnij} + \boldsymbol{f}_{Ctij}\right) \tag{4.21}$$

$$\boldsymbol{T}_{Ci} = \sum_j \left(r_s \boldsymbol{n}_{ij} \times \boldsymbol{f}_{Ctij}\right) \tag{4.22}$$

4.2.2.1 Time step

The time step should be set smaller than a certain critical value in order to make the calculation stable. However, the time step should be as large as possible to save computation time. Therefore, a suitable time step should be chosen. There are two kinds of time step must be considered. The time step requires for calculating particle motion and fluid motion. From the viewpoint of the stability of calculation, the critical time step for particle motion is much less than that of fluid motion. Cundall and Strack (1979) proposed a method for determining the time step for calculating particle motion, which is based on the characteristic natural frequency of a spring-mass oscillation system. Reffering to their method, the time step is determined by the following procedure. First, we randomly distributed the particles in the vessel as the initial condition according to a uniform probability distribution. Fluid motion was neglected. Using the DEM, we calculated the motion of these particles

falling from the initial still condition under the effect of gravity and neglecting interaction with the fluid. The oscillation period of the spring-mass system used to model contacting particles is given by

$$\tau = 2\pi\sqrt{m/k} \tag{4.23}$$

One half of the above period was divided by a factor of n to obtain the time stime step. Tsujj et. al.(1993) investigate a suitable n for time step. They found that a suitable n is 5.

Therefore, the time step is as follow.

$$\tau = \frac{\pi\sqrt{m/k}}{5} \tag{4.24}$$

4.2.2.2 Stiffness or Spring Constant

The stiffness can be determined from the material properties with Hertzian theory. When the Cundall's model is applied to a sand or snow avalanche, it is not practicable to take the smallest sand or snow particle as the distinct element but a particle assembly of suitable size should be taken as one particle (virtual particle) because of the limit of memory size and computation time. In such a case, the stiffness of the virtual particle is expected to be smaller than that of an actual particle. It is often difficult in practice to use the stiffness calculated by Hertzian theory, because the time step required for numerical integration becomes so small that an excessive amount of computational time is needed. The time step should be less than one-tenth of the natural oscillation period $2\pi\sqrt{m/k}$ of a spring-mass system. Therefore, a small value of stiffness is assumed for convenience of the calculation.

4.2.3 Fluid motion

The locally averaged equation of continuity and equations of motion were used for the calculation of the fluid motion. The finite difference method was used

to calculate fluid motion. The flow domain was divided into cells, the size of which is larger than the particle size. All quantities such as pressure and fluid velocity are averaged in the cell. The void fraction of each cell can be defined as the number of particles existing in the cell. The basic equations are as follows.

Equation of continuity

$$\frac{\partial}{\partial t}\varepsilon + \frac{\partial}{\partial x_j}\left(\varepsilon u_j\right) = 0 \tag{4.25}$$

Equation of motion

$$\frac{\partial}{\partial t}\left(\varepsilon u_i\right) + \frac{\partial}{\partial x_j}\left(\varepsilon u_i u_j\right) = -\frac{\varepsilon}{\rho_g}\frac{\partial p}{\partial x_i} + f_{pi} \tag{4.26}$$

where ε, u, p and ρ_g are the void fraction, fluid velocity, pressure and fluid density, respectively. Fluid is treated as inviscid except the interaction term (f_{pi}) between the fluid and particles.

$$f_{pi} = \frac{\beta}{\rho_g}\left(\bar{v}_{pi} - u_i\right) \tag{4.27}$$

where $\bar{v}_{pi}$ is the average particle velocities. The coefficient β is derived from Ergun's equation for dense phase and Wen and Yu's equation for dilute phase.

$$\beta = \begin{cases} \dfrac{\mu(1-\varepsilon)}{d_p^2\varepsilon}\left[150(1-\varepsilon)+1.75Re\right] & (\varepsilon \le 0.8) \\ \dfrac{3}{4}C_D\dfrac{\mu(1-\varepsilon)}{d_p^2}\varepsilon^{-2.7}Re & (\varepsilon > 0.8) \end{cases} \tag{4.28}$$

$$C_D = \begin{cases} 24\left(1+0.15Re^{0.687}\right)/Re & (Re \le 1000) \\ 0.43 & (Re > 1000) \end{cases} \tag{4.29}$$

$$Re = \frac{\left|\boldsymbol{v}_p - \boldsymbol{u}\right|\rho_g \varepsilon d_p}{\mu_g} \tag{4.30}$$

where C_D is the drag coefficient for a single sphere, d_p is the particle diameter, and μ is the viscosity.

4.3 Numerical technique

Finite difference method used to solve PDE in this work. The concept of the finite difference method is shown in this section. Most common finite-difference representations of derivatives are based on Taylor's series expansions. For example, referring to Figure 10, if $u_{i,j}$ denotes the x component of velocity at point (i,j), then the velocity $u_{i+1,j}$ at point $(i+1,j)$ can be expressed in terms of a Taylor series expanded about point (i, j) as follows:

$$u_{i+1,j} = u_{i,j} + \left(\frac{\partial u}{\partial x}\right)_{i,j} \Delta x + \left(\frac{\partial^2 u}{\partial x^2}\right)_{i,j} \frac{(\Delta x)^2}{2} + \left(\frac{\partial^3 u}{\partial x^3}\right)_{i,j} \frac{(\Delta x)^3}{6} + \ldots \qquad (4.31)$$

Equation (4.31) is mathematically an exact expression for u_{i+1},j if (1) the number of terms is infinite and the series converges and/or (2) $\Delta x \rightarrow 0$. Solving Equation (1) for $(\partial u / \partial x)_{i,j}$, we obtain

$$\left(\frac{\partial u}{\partial x}\right)_{i,j} = \frac{u_{i+1,j} - u_{i,j}}{\Delta x} - \left(\frac{\partial^2 u}{\partial x^2}\right)_{i,j} \frac{\Delta x}{2} - \left(\frac{\partial^3 u}{\partial x^3}\right)_{i,j} \frac{(\Delta x)^2}{6} + \ldots \qquad (4.32)$$

Finite difference representation

Truncation error

In Equation (4.32), the actual partial derivative at point (i, j) is given on the left side. The first term on the right side is a finite-difference representation of the partial derivative. The remaining terms on the right side constitute the truncation error. That is, if we wish to approximate the partial derivative with the above algebraic finite-difference quotient,

$$\left(\frac{\partial u}{\partial x}\right)_{i,j} \approx \frac{u_{i+1,j} - u_{i,j}}{\Delta x} \qquad (4.33)$$

I21595884

then, the truncation error in Equation (4.32) tells us what is being neglected in this approximation. In Equation (4.32), the lowest-order term in the truncation error involves Δx to the first power; hence, the finite-difference expression in Equation(4.33) is called first-order-accurate. We can more formally write Equation (4.32) as

$$\left(\frac{\partial u}{\partial x}\right)_{i,j} = \frac{u_{i+1,j} - u_{i,j}}{\Delta x} + O(\Delta x) \tag{4.34}$$

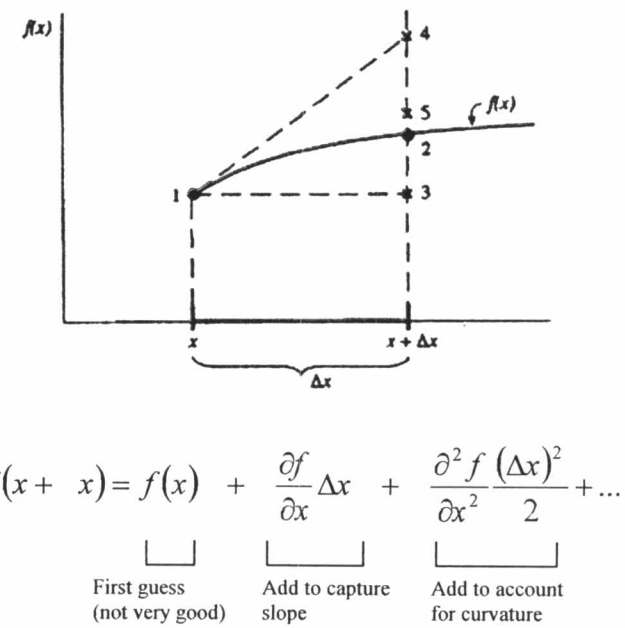

$$f(x + x) = f(x) + \frac{\partial f}{\partial x}\Delta x + \frac{\partial^2 f}{\partial x^2}\frac{(\Delta x)^2}{2} + \ldots$$

First guess (not very good) | Add to capture slope | Add to account for curvature

Figure 4.3 Illustration of the first three terms in a Taylor series

In Equation (4.34), the symbol O(Δx) is a formal mathematical notation which represents "terms of order Δx" Equation (4.34) is a more precise notion than Equation (4.33), which involves the "approximately equal" notion; in Equation (4.34) the order of magnitude of the truncation error is shown explicitly by the notion. Also referring to Fig.1, note that the finite-difference expression in Equation (4.34) uses information to the right of grid point (*i,j*); that is, it uses u_{i+1},j as well as u_{ij}. No information to the left of (*i,j*) is used. As a result, the finite difference in Equation (4.34) is called a forward difference. For this reason, we now identify the first-order-accurate difference representation for the derivative

$(\partial u/\partial x)_{i,j}$ expressed by Equation (4.34) as a first-order forward difference, repeated below

$$\left(\frac{\partial u}{\partial x}\right)_{i,j} = \frac{u_{i+1,j} - u_{i,j}}{\Delta x} + O(\Delta x)$$

Let us now write a Taylor series expansion for $u_{i-1,j}$, expanded about $u_{i,j}$.

$$u_{i-1,j} = u_{i,j} + \left(\frac{\partial u}{\partial x}\right)_{i,j}(-\Delta x) + \left(\frac{\partial^2 u}{\partial x^2}\right)_{i,j}\frac{(-\Delta x)^2}{2} + \left(\frac{\partial^3 u}{\partial x^3}\right)_{i,j}\frac{(-\Delta x)^3}{6} + \ldots \quad (4.35)$$

or

$$u_{i-1,j} = u_{i,j} - \left(\frac{\partial u}{\partial x}\right)_{i,j}\Delta x + \left(\frac{\partial^2 u}{\partial x^2}\right)_{i,j}\frac{(\Delta x)^2}{2} - \left(\frac{\partial^3 u}{\partial x^3}\right)_{i,j}\frac{(\Delta x)^3}{6} + \ldots \quad (4.36)$$

Solving for $(\partial u/\partial x)_{i,j}$, we obtain

$$\left(\frac{\partial u}{\partial x}\right)_{i,j} = \frac{u_{i,j} - u_{i-1,j}}{\Delta x} + O(\Delta x) \quad (4.37)$$

The information used in forming the finite-difference quotient in Equation (4.37) comes from the left of grid point (i,j); that is, it uses $u_{i-1,j}$ as well as $u_{i,j}$. No information to the right of (i,j) is used. As a result, the finite difference in Equation (4.36) is called a rearward (or backward) difference. Moreover, the lowest-order term in the truncation error involves Δx to the first power. As a result, the finite difference in Equation (4.36) is called a first – order rearward difference.

In most application in computational fluid dynamic (CFD), first-order accuracy is not sufficient. To construct a finite-difference quotient of second-order accuracy, simply subtract Equation (4.35) from Equation (4.31):

$$u_{i+1,j} - u_{i-1,j} = 2\left(\frac{\partial u}{\partial x}\right)_{i,j}\Delta x + 2\left(\frac{\partial^3 u}{\partial x^3}\right)_{i,j}\frac{(\Delta x)^3}{6} + \ldots \quad (4.38)$$

Equation (4.38) can be written as

$$\left(\frac{\partial u}{\partial x}\right)_{i,j} = \frac{u_{i+1,j} - u_{i-1,j}}{2\Delta x} + O(\Delta x)^2 \tag{4.39}$$

The information used in forming the finite-difference quotient in Equation (4.38) comes from both sides of the grid point located at (*i,j*); that is, it uses $u_{i+1,j}$ as well as $u_{i-1,j}$. Grid point (*i,j*) falls between the two adjacent grid point. Moreover in truncation error in Equation (4.37), the lowest-order terms involves $(\Delta x)^2$,which is second order accuracy. Hence, the finite-difference quotient in Equation (4.38) is called a second order central difference.

Difference expressions for the y derivatives are obtained in exactly the same fashion. The results are directly analogy to the previous equations for the x derivatives. They are:

$$\left(\frac{\partial u}{\partial y}\right)_{i,j} = \begin{cases} \dfrac{u_{i,j+1} - u_{i,j}}{\Delta y} + O(\Delta y) & \textit{Forward difference} \\ \dfrac{u_{i,j} - u_{i,j-1}}{\Delta y} + O(\Delta y) & \text{Re}\textit{arward difference} \\ \dfrac{u_{i,j+1} - u_{i,j-1}}{2\Delta y} + O(\Delta y)^2 & \textit{Central difference} \end{cases} \tag{4.40}$$

Equation (4.40) is the equation of finite-difference quotients for first partial derivatives. If we are dealing with inviscid flows only, the governing equations are the Euler equations. Note that that highest-order derivatives which appear in the Euler equations are first partial derivatives. Hence, finite differences for the first derivatives use for the numerical solution of inviscid flows. On the other hand, if we are dealing with viscous flows, the governing equations are the Navier-Stokes equations. Note that the highest-order derivatives which appear in the Navier-Stokes equations are second partial derivatives. Consequently, there is a need for discretizing second-order derivatives for CFD. We can obtain such finite-difference expressions by continuing with a Taylor series analysis, as

follows. Summing the Taylor series expansions given by Equations (4.31) and (4.35), we have

$$u_{i+1,j} + u_{i-1,j} = 2u_{i,j} + \left(\frac{\partial^2 u}{\partial x^2}\right)_{i,j} (\Delta x)^2 + \left(\frac{\partial^4 u}{\partial x^4}\right)_{i,j} \frac{(\Delta x)^4}{12} + \ldots \tag{4.41}$$

Solving for $\left(\partial^2 u / \partial x\right)_{i,j}$,

$$\left(\frac{\partial^2 u}{\partial x^2}\right)_{i,j} = \frac{u_{i+1,j} - 2u_{i,j} + u_{i-1,j}}{(\Delta x)^2} + O(\Delta x)^2 \tag{4.42}$$

In Equation (4.42), the first term on the right-hand side is a central finite difference for the second derivative with respect to *x* evaluated at grid point (*i,j*); from the remaining order-of-magnitude term, we see that this central difference is of second-order accuracy. An analogous expression can easily be obtained for the second derivative with respect to *y*, with the result that

$$\left(\frac{\partial^2 u}{\partial y^2}\right)_{i,j} = \frac{u_{i,j+1} - 2u_{i,j} + u_{i,j-1}}{(\Delta y)^2} + O(\Delta y)^2 \tag{4.43}$$

Equations (4.42) and (4.43) are examples of second-order central second differences. For the case of mixed derivatives, such as $\partial^2 u / \partial x \partial y$, appropriate finite-difference quotients is:

$$\left(\frac{\partial^2 u}{\partial x \partial y}\right)_{i,j} = \frac{u_{i+1,j+1} - u_{i+1,j-1} - u_{i-1,j+1} + u_{i-1,j-1}}{4\Delta x \Delta y} + O\left[(\Delta x)^2, (\Delta y)^2\right] \tag{4.44}$$

Equation (4.44) gives a second-order central difference for the mixed derivative, $\left(\partial^2 u / \partial x \partial y\right)_{i,j}$

4.3.1 Staggered grid

The staggered grid for the velocity components was first used by Harlow and Welch(1965) in their MAC method and has been used in other methods developed by Harlow and co-workers. It forms the basis of the SIVA procedure of Caretto, Curr, and Spalding (1972) and the SIMPLE procedure of Patankar and Spalding (1972).

In the staggered grid, the velocity components are calculated for the points that lie on the faces of the control volumes. It is easy to see how the locations for the velocity components v and w are to be defined. In Figure 4.4, a two-dimensional grid pattern is shown, with the locations for *v* and *w* placed on the respective control-volume faces.

The important advantages are twofold. For a typical control volume (shown in Figure 4.4), it is easy to see that the discretized continuity equation would contain the differences of adjacent velocity components, and that is would prevent a wavy velocity field from satisfying the continuity equation. The second important advantage of the staggered grid is that the pressure difference between two adjacent grid points now becomes the natural driving force for the velocity component located between these grid points.

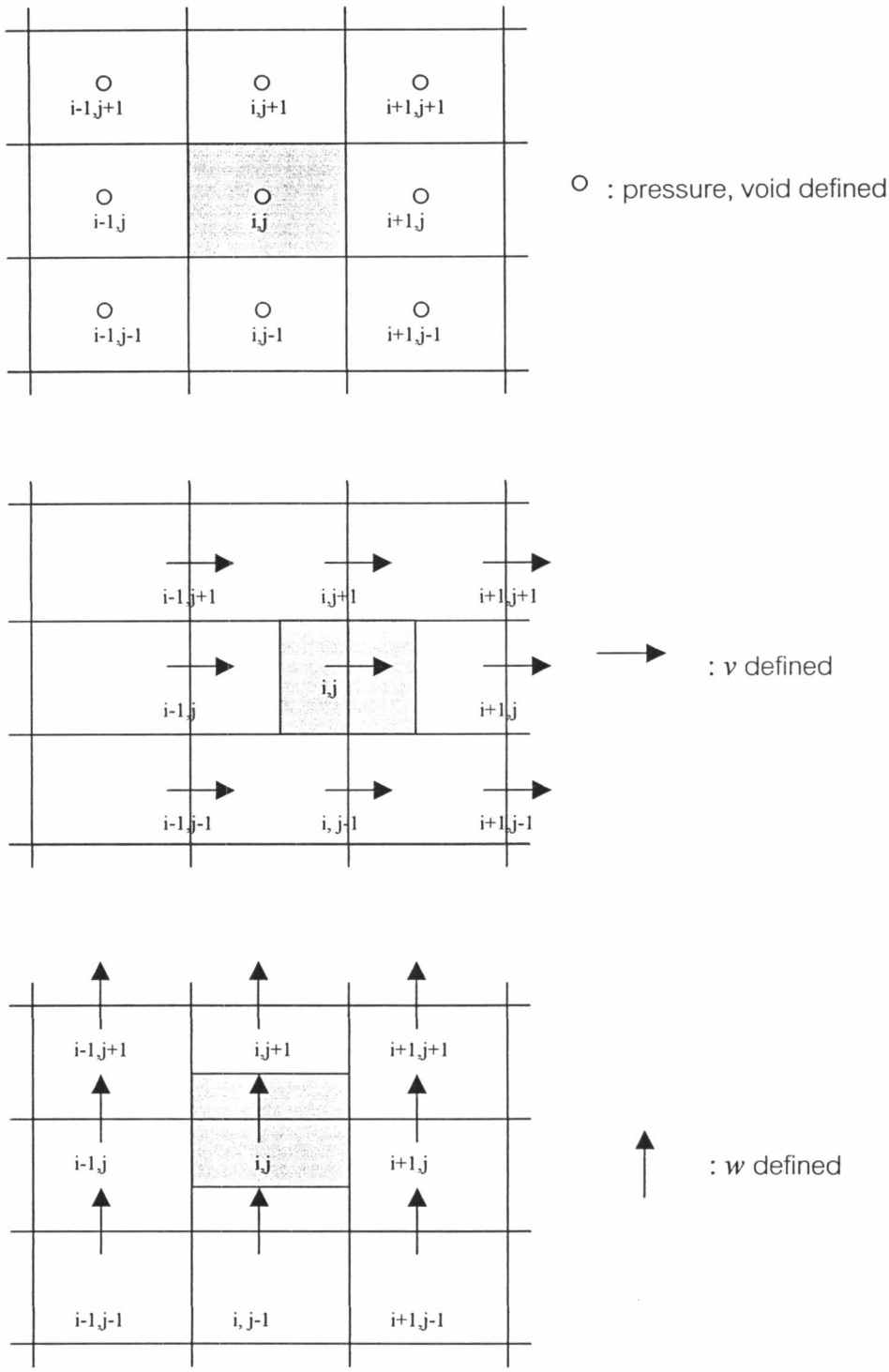

Figurer 4.4 Staggered locations for pressure, void, *v* and *w*

4.3.2 Discretization method

A numerical solution of a differential equation consists of a set of numbers from which the distribution of the dependent variable ϕ can be constructed. A numerical method treats as its basic unknowns the values of the dependent variable at a finite number of locations (called the points) in the calculation domain. The method includes the tasks of providing a set of algebraic equations for these unknowns and of prescribing an algorithm for solving the equations. In focusing attention on the values at the grid points, we have replaced the continuous information contained in the exact solution the differential equation with discrete values. We have thus discretized the distribution of ϕ, and it is appropriate to refer to this class of numerical methods as discretization methods.

From Equation (4.25), the continuity equation can be written as

$$\frac{\partial}{\partial t}\varepsilon+\frac{\partial}{\partial y}(\varepsilon v)+\frac{\partial}{\partial z}(\varepsilon w)=0 \tag{4.45}$$

From Equation (4.26), the equation of motion can be written as

In y-direction

$$\frac{\partial}{\partial t}(\varepsilon v)+\frac{\partial}{\partial y}(\varepsilon vv)+\frac{\partial}{\partial z}(\varepsilon vw)=-\frac{\varepsilon}{\rho}\frac{\partial p}{\partial y}+\frac{K_y}{\rho} \tag{4.46}$$

In z-direction

$$\frac{\partial}{\partial t}(\varepsilon w)+\frac{\partial}{\partial y}(\varepsilon vw)+\frac{\partial}{\partial z}(\varepsilon ww)=-\frac{\varepsilon}{\rho}\frac{\partial p}{\partial y}+\frac{K_z}{\rho} \tag{4.47}$$

4.3.2.1 Discretization of momentum equations

Discretization of momentum equations (Equation 4.46) in y-direction

$$\frac{\partial}{\partial t}(\varepsilon v)+\frac{\partial}{\partial y}(\varepsilon vv)+\frac{\partial}{\partial z}(\varepsilon vw)=-\frac{\varepsilon}{\rho}\frac{\partial p}{\partial y}+\frac{K_y}{\rho}$$

Integrate the equation of motion (Equation 4.46) in the control volume as shown in Figure 4.5.

$$\int_w^e \int_s^n \int_t^{t+\Delta t} \frac{\partial}{\partial t}(\varepsilon v)dtdydz + \int_t^{t+\Delta t} \int_s^n \int_w^e \frac{\partial}{\partial y}(\varepsilon vv)dydzdt + \int_t^{t+\Delta t} \int_w^e \int_s^n \frac{\partial}{\partial z}(\varepsilon vw)dzdydt$$

$$= \int_t^{t+\Delta t} \int_s^n \int_w^e \left(-\frac{\varepsilon}{\rho}\frac{\partial p}{\partial y} \right) dydzdt + \frac{K_y}{\rho}\Delta y \Delta z \Delta t$$

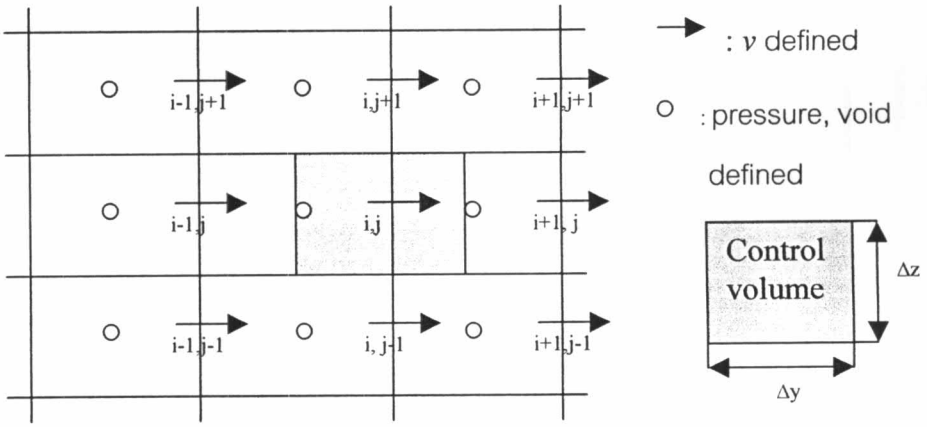

Figure 4.5 Control volume for calculating *v*

$$\int_w^e \int_s^n \int_t^{t+\Delta t} \frac{\partial}{\partial t}(\varepsilon v)dtdydz = \left\{ (\varepsilon v)_p - (\varepsilon v)_p^0 \right\} \Delta y \Delta z$$

where $(\ )^0$ is value at time t

$$\int_t^{t+\Delta t} \int_s^n \int_w^e \frac{\partial}{\partial y}(\varepsilon vv)dydzdt = (\varepsilon vv)_e \Delta z \Delta t - (\varepsilon vv)_w \Delta z \Delta t = J_e \Delta t - J_w \Delta t$$

$$[\varepsilon vv]_{e-w} = (\varepsilon vv)_e - (\varepsilon vv)_w$$

$$\int_t^{t+\Delta t} \int_w^e \int_s^n \frac{\partial}{\partial z}(\varepsilon vw)dzdydt = (\varepsilon vw)_n \Delta y \Delta t - (\varepsilon vw)_s \Delta y \Delta t = J_n \Delta t - J_s \Delta t$$

$$[\varepsilon vw]_{n-s} = (\varepsilon vw)_n - (\varepsilon vw)_s$$

$$\int_{t}^{t+\Delta t}\int_{s}^{n}\iint_{w}^{e}\left(-\frac{\varepsilon}{\rho}\frac{\partial p}{\partial y}\right)dydzdt=\frac{\varepsilon_p}{\rho}(p_E-p_P)\Delta z\Delta t$$

$$\frac{\varepsilon_p}{\rho}[p]_{e-w}=\frac{\varepsilon_p}{\rho}(p_e-p_w)=\frac{\varepsilon_p}{\rho}(p_E-p_P)$$

$$\left\{\frac{(\varepsilon v)_p-(\varepsilon v)_p^0}{\Delta t}\right\}\Delta y\Delta z+J_e-J_w+J_n-J_s=-\frac{\varepsilon_p}{\rho}(p_E-p_P)\Delta z+\frac{K_y}{\rho}\Delta y\Delta z$$

Integrate the equation of continuity in the same control volume (Control volume for v)

$$\frac{\partial}{\partial t}\varepsilon+\frac{\partial}{\partial y}(\varepsilon v)+\frac{\partial}{\partial z}(\varepsilon w)=0$$

$$\left\{\frac{\varepsilon_p-\varepsilon_p^0}{\Delta t}\right\}\Delta y\Delta z+F_e-F_w-F_n-F_s=0$$

$$\frac{\Delta y\Delta z}{\Delta t}\varepsilon_p^0(v_p-v_p^0)+(J_e-v_pF_e)-(J_w-v_pF_w)+(J_n-v_pF_n)-(J_s-v_pF_s)$$
$$=-\frac{\varepsilon}{\rho}(p_E-p_p)\Delta z+\frac{K_y}{\rho}\Delta y\Delta z$$

where

$$J_e=(\varepsilon vv)_e\Delta z,\quad J_w=(\varepsilon vv)_w\Delta z,\quad J_n=(\varepsilon wv)_n\Delta y,\quad J_s=(\varepsilon wv)_s\Delta y$$

$$F_e=(\varepsilon v)_e\Delta z=\varepsilon_e v_e\Delta z=\varepsilon_{i+1,j}\frac{v_{i,j}+v_{i+1,j}}{2}\Delta z$$

$$F_w=(\varepsilon v)_w\Delta z=\varepsilon_w v_w\Delta z=\varepsilon_{i,j}\frac{v_{i,j}+v_{i-1,j}}{2}\Delta z$$

$$F_n=(\varepsilon w)_n\Delta y=\varepsilon_n w_n\Delta y=\frac{\varepsilon_{i,j}+\varepsilon_{i+1,j}+\varepsilon_{i,j+1}+\varepsilon_{i+1,j+1}}{4}\frac{w_{i,j}+w_{i+1,j}}{2}$$

$$F_s=(\varepsilon w)_s\Delta y=\varepsilon_s w_s\Delta y=\frac{\varepsilon_{i,j}+\varepsilon_{i+1,j}+\varepsilon_{i,j+1}+\varepsilon_{i+1,j+1}}{4}\frac{w_{i,j-1}+w_{i+1,j-1}}{2}$$

$$J_e=(\varepsilon vv)_e\Delta z=(\varepsilon v)_e\Delta z\cdot v_e=F_e\cdot v_e\quad,$$

F_e = flow rate through e-surface as shown in Figure 4.5

For v_e use upwind method Fe > 0, $v_e = v_{i,j}$ or Fe < 0, ve = $v_{i+1,j}$

$$J_e = F_e \cdot v_e = v_{i,j} \max[F_e,0] - v_{i+1,j} \max[-F_e,0]$$

$$v_p F_e = v_{i,j} \max[F_e,0] - v_{i,j} \max[-F_e,0]$$

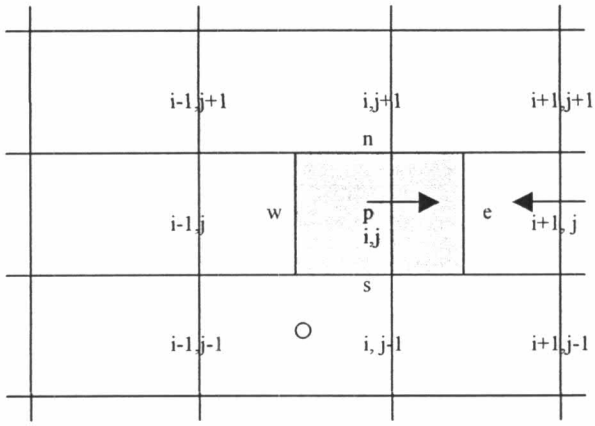

Figure 4.6 Surface of control volume for *v*

Therefore

$$J_e - v_p F_e = \max[-F_e,0](v_{i,j} - v_{i+1,j}) = a_e(v_{i,j} - v_{i+1,j})$$
$$J_w - v_p F_w = \max[F_w,0](v_{i-1,j} - v_{i,j}) = a_w(v_{i-1j} - v_{i,j})$$
$$J_n - v_p F_n = \max[-F_n,0](v_{i,j} - v_{i,j+1}) = a_n(v_{i,j} - v_{i,j+1})$$
$$J_s - v_p F_s = \max[F_s,0](v_{i,j-1} - v_{i,j}) = a_s(v_{i,j-1} - v_{i,j})$$

$$a_p v_{i,j} = a_e v_{i+1,j} + a_w v_{i-1,j} + a_n v_{i,j+1} + a_s v_{i,j-1} + b_y + \frac{1}{\rho}\frac{\varepsilon_{i,j} + \varepsilon_{i+1,j}}{2}\left(p_{i,j} - p_{i+1,j}\right)\Delta z \tag{4.48}$$

where $a_p = a_e + a_w + a_n + a_s + \dfrac{\Delta y \Delta z}{\Delta t}\dfrac{\varepsilon^0_{i,j} + \varepsilon_{i+1,j}}{2}$

$$b_y = \frac{\Delta y \Delta z}{\Delta t}\frac{\varepsilon^0_{i,j} + \varepsilon^0_{i+1,j}}{2} v^0_{i,j} + \frac{K_{yi,j}}{\rho}\Delta y \Delta z$$

Discretization of momentum equations (Equation (4.47)) in z-direction in the same way

$$\frac{\partial}{\partial t}(\varepsilon w)+\frac{\partial}{\partial y}(\varepsilon v w)+\frac{\partial}{\partial z}(\varepsilon w w)=-\frac{\varepsilon}{\rho}\frac{\partial p}{\partial y}+\frac{K_z}{\rho}$$

Integrate the equation of motion in the control volume as shown in Figure 4.7.

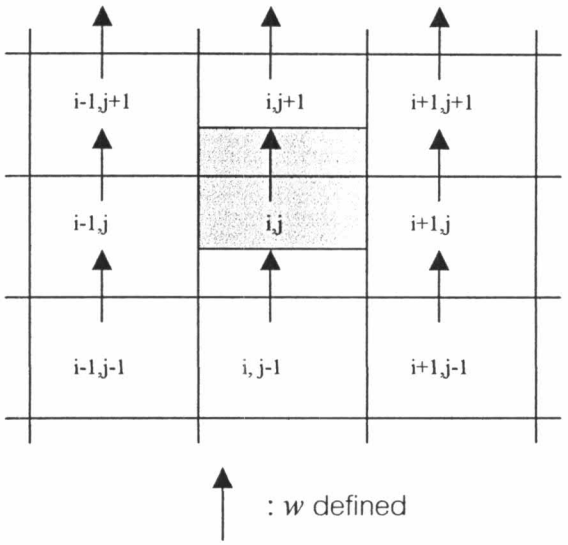

Figure 4.7 Surface of control volume for w

$$a_p w_{i,j} = a_e w_{i+1,j} + a_w w_{i-1,j} + a_n w_{i,j+1} + a_s w_{i,j-1} + b_z + \frac{1}{\rho}\frac{\varepsilon_{i,j}+\varepsilon_{i+1,j}}{2}\left(p_{i,j}-p_{i+1,j}\right)\Delta y \tag{4.49}$$

where $a_p = a_e + a_w + a_n + a_s + \dfrac{\Delta y \Delta z}{\Delta t}\dfrac{\varepsilon^0_{i,j}+\varepsilon^0_{i+1,j}}{2}$

$$b_z = \frac{\Delta y \Delta z}{\Delta t}\frac{\varepsilon^0_{i,j}+\varepsilon^0_{i+1,j}}{2} w^0_{i,j} + \frac{K_{zi,j}}{\rho}\Delta y \Delta z$$

$$a_e = \max[-F_e,0],\quad a_w = \max[F_w,0],\quad a_n = \max[-F_n,0],\quad a_s = \max[F_s,0]$$

$$F_e = (\varepsilon v)_e \Delta z = \frac{\varepsilon_{i,j}+\varepsilon_{i+1,j}+\varepsilon_{i,j+1}+\varepsilon_{i+1,j+1}}{4}\frac{v_{i,j}+v_{i+1,j}}{2}\Delta z$$

$$F_w = (\varepsilon v)_w \Delta z = \frac{\varepsilon_{i,j}+\varepsilon_{i-1,j}+\varepsilon_{i,j+1}+\varepsilon_{i-1,j+1}}{4}\frac{v_{i-1,j}+v_{i-1,j+1}}{2}\Delta z$$

$$F_n = (\varepsilon w)_n \Delta y = \varepsilon_{i,j+1}\frac{w_{i,j}+w_{i,j+1}}{2}\Delta y$$

$$F_s = (\varepsilon w)_s \Delta y = \varepsilon_{i,j+1}\frac{w_{i,j}+w_{i,j-1}}{2}\Delta y$$

Summary of discretization of momentum equations

In y-direction

$$a_p v_{i,j} = a_e v_{i+1,j} + a_w v_{i-1,j} + a_n v_{i,j+1} + a_s v_{i,j-1} + b_y + \frac{1}{\rho}\frac{\varepsilon_{i,j} + \varepsilon_{i+1,j}}{2}\left(p_{i,j} - p_{i+1,j}\right)\Delta z$$

$$a_{py\,i,j} v_{i,j} = \sum av + b_y + \frac{1}{\rho}\frac{\varepsilon_{i,j} + \varepsilon_{i+1,j}}{2}\left(p_{i,j} - p_{i+1,j}\right)\Delta z \qquad (4.50)$$

where $a_p = a_{py\,i,j}$

$$\sum av = a_e v_{i+1,j} + a_w v_{i-1,j} + a_n v_{i,j+1} + a_s v_{i,j-1}$$

In z-direction

$$a_p w_{i,j} = a_e w_{i+1,j} + a_w w_{i-1,j} + a_n w_{i,j+1} + a_s w_{i,j-1} + b_z + \frac{1}{\rho}\frac{\varepsilon_{i,j} + \varepsilon_{i+1,j}}{2}\left(p_{i,j} - p_{i+1,j}\right)\Delta y$$

$$a_{pz\,i,j} w_{i,j} = \sum aw + b_z + \frac{1}{\rho}\frac{\varepsilon_{i,j} + \varepsilon_{i+1,j}}{2}\left(p_{i,j} - p_{i,j+1}\right)\Delta y \qquad (4.51)$$

where $a_p = a_{pz\,i,j}$

$$\sum aw = a_e w_{i+1,j} + a_w w_{i-1,j} + a_n w_{i,j+1} + a_s w_{i,j-1}$$

4.3.2.2 Discretization of continuity equation

$$\frac{\partial}{\partial t}\varepsilon + \frac{\partial}{\partial y}(\varepsilon v) + \frac{\partial}{\partial z}(\varepsilon w) = 0$$

Integrate the continuity equation in the control volume as shown in Figure 4.8

$$\int_w^e \int_s^n \int_t^{t+\Delta t} \frac{\partial}{\partial t}(\varepsilon)\,dt\,dy\,dz + \int_t^{t+\Delta t} \int_s^n \int_w^e \frac{\partial}{\partial y}(\varepsilon v)\,dy\,dz\,dt + \int_t^{t+\Delta t} \int_w^e \int_s^n \frac{\partial}{\partial z}(\varepsilon w)\,dz\,dy\,dt = 0$$

$$\frac{\Delta y \Delta z}{\Delta t}\left(\varepsilon_{i,j}-\varepsilon_{i,j}^{0}\right)+\frac{\varepsilon_{i,j}+\varepsilon_{i+1,j}}{2}v_{i,j}\Delta z-\frac{\varepsilon_{i,j}+\varepsilon_{i-1,j}}{2}v_{i-1,j}\Delta z+\frac{\varepsilon_{i,j}+\varepsilon_{i,j+1}}{2}w_{i,j}\Delta y$$
$$-\frac{\varepsilon_{i,j}+\varepsilon_{i,j-1}}{2}w_{i,j-1}=0 \qquad (4.52)$$

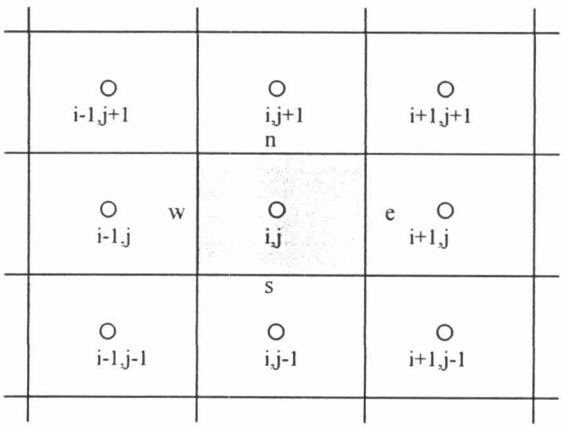

Figure 4.8 Surface of control volume for continuity equation

4.3.2.3 Modify pressure and velocity

$$v = v^{*} + v'$$
$$w = w^{*} + w'$$
$$p = p^{*} + p'$$

where v^{*}, w^{*}, p^{*} are assumed values

v', w', p' are modified value

In y-direction

$$a_{py\,i,j}v_{i,j} = \sum av + b_y + \frac{1}{\rho}\frac{\varepsilon_{i,j}+\varepsilon_{i+1,j}}{2}\left(p_{i,j}-p_{i+1,j}\right)\Delta z \qquad (4.53)$$

Substitute assumed value into Equation (4.53)

$$a_{py\,i,j}v^{*}_{i,j} = \sum av^{*} + b_y + \frac{1}{\rho}\frac{\varepsilon_{i,j}+\varepsilon_{i+1,j}}{2}\left(p^{*}_{i,j}-p^{*}_{i+1,j}\right)\Delta z \qquad (4.54)$$

Equation (4.53)-Equation (4.54)

$$a_{py\,i,j}v'_{i,j} = \sum av' + \frac{1}{\rho}\frac{\varepsilon_{i,j} + \varepsilon_{i+1,j}}{2}\left(p'_{i,j} - p'_{i+1,j}\right)\Delta z$$

Neglecting $\sum av'$

$$v'_{i,j} = \frac{1}{a_{py\,i,j}\rho}\frac{\varepsilon_{i,j} + \varepsilon_{i+1,j}}{2}\left(p'_{i,j} - p'_{i+1,j}\right)\Delta z \tag{4.55}$$

In z-direction

$$a_{pz\,i,j}w_{i,j} = \sum aw + b_z + \frac{1}{\rho}\frac{\varepsilon_{i,j} + \varepsilon_{i+1,j}}{2}\left(p_{i,j} - p_{i,j+1}\right)\Delta y \tag{4.56}$$

Substitute assumed value into Equation (4.56)

$$a_{pz\,i,j}w^*_{i,j} = \sum aw^* + b_z + \frac{1}{\rho}\frac{\varepsilon_{i,j} + \varepsilon_{i+1,j}}{2}\left(p^*_{i,j} - p^*_{i,j+1}\right)\Delta y \tag{4.57}$$

Equation (4.56)-Equation (4.57)

$$a_{pz\,i,j}w'_{i,j} = \sum aw' + \frac{1}{\rho}\frac{\varepsilon_{i,j} + \varepsilon_{i+1,j}}{2}\left(p'_{i,j} - p'_{i,j+1}\right)\Delta y$$

Neglecting $\sum aw'$

$$w'_{i,j} = \frac{1}{a_{pz\,i,j}\rho}\frac{\varepsilon_{i,j} + \varepsilon_{i+1,j}}{2}\left(p'_{i,j} - p'_{i,j+1}\right)\Delta y \tag{4.58}$$

Substitute Equation (4.55) and Equation (4.58) in $v = v^* + v'$ and $w = w^* + w'$

$$v_{i,j} = v^*_{i,j} + v'_{i,j} = v^*_{i,j} + \frac{1}{a_{py\,i,j}\rho}\frac{\varepsilon_{i,j} + \varepsilon_{i+1,j}}{2}\left(p'_{i,j} - p'_{i+1,j}\right)\Delta z \tag{4.59}$$

$$w_{i,j} = w^*_{i,j} + w'_{i,j} = w^*_{i,j} + \frac{1}{a_{pz\,i,j}\rho}\frac{\varepsilon_{i,j} + \varepsilon_{i+1,j}}{2}\left(p'_{i,j} - p'_{i,j+1}\right)\Delta y \tag{4.60}$$

Substitute Equation (4.59) and Equation (4.60) in Equation (4.52)

$$c_p p'_{i,j} = c_e p'_{i+1,j} + c_w p'_{i-1,j} + c_n p'_{i,j+1} + c_s p'_{i,j-1} + b \tag{4.61}$$

where

$$c_p = c_e + c_w + c_n + c_s$$

$$c_e = \frac{1}{a_{py\,i,j}\rho}\left(\frac{\varepsilon_{i,j} + \varepsilon_{i+1,j}}{2}\right)^2 \Delta z^2$$

$$c_w = \frac{1}{a_{py\,i-1,j}\rho}\left(\frac{\varepsilon_{i,j} + \varepsilon_{i-1,j}}{2}\right)^2 \Delta z^2$$

$$c_n = \frac{1}{a_{pz\,i,j}\rho}\left(\frac{\varepsilon_{i,j} + \varepsilon_{i+1,j}}{2}\right)^2 \Delta y^2$$

$$c_s = \frac{1}{a_{pz\,i,j-1}\rho}\left(\frac{\varepsilon_{i,j} + \varepsilon_{i,j-1}}{2}\right)^2 \Delta y^2$$

$$b = \frac{\Delta y \Delta z}{\Delta t}\left(\varepsilon_{i,j} - \varepsilon_{i,j}^0\right) - \frac{\varepsilon_{i,j} + \varepsilon_{i+1,j}}{2} v_{i,j}^* \Delta z + \frac{\varepsilon_{i,j} + \varepsilon_{i-1,j}}{2} v_{i-1,j}^* \Delta z - \frac{\varepsilon_{i,j} + \varepsilon_{i,j+1}}{2} w_{i,j}^* \Delta y + \frac{\varepsilon_{i,j} + \varepsilon_{i,j-1}}{2} w_{i,j-1}^* \Delta y \tag{4.62}$$

If v* and w* are correct, b=0. If b≠0, modification p' is obtained from Equation (4.61). The algorithm of modify pressure and velocity is shown in Figure 4.9.

4.3.2.4 Relaxation factor

The modify pressure is prone to diverge unless some relaxation is used

$$p = p^* + \alpha_R p' \tag{4.63}$$

where α_R is a relaxation factor. When the relaxation factor is between 0 and 1, its effect is underrelaxation. When the relaxation factor is greater than 1, overrelaxation is produced.

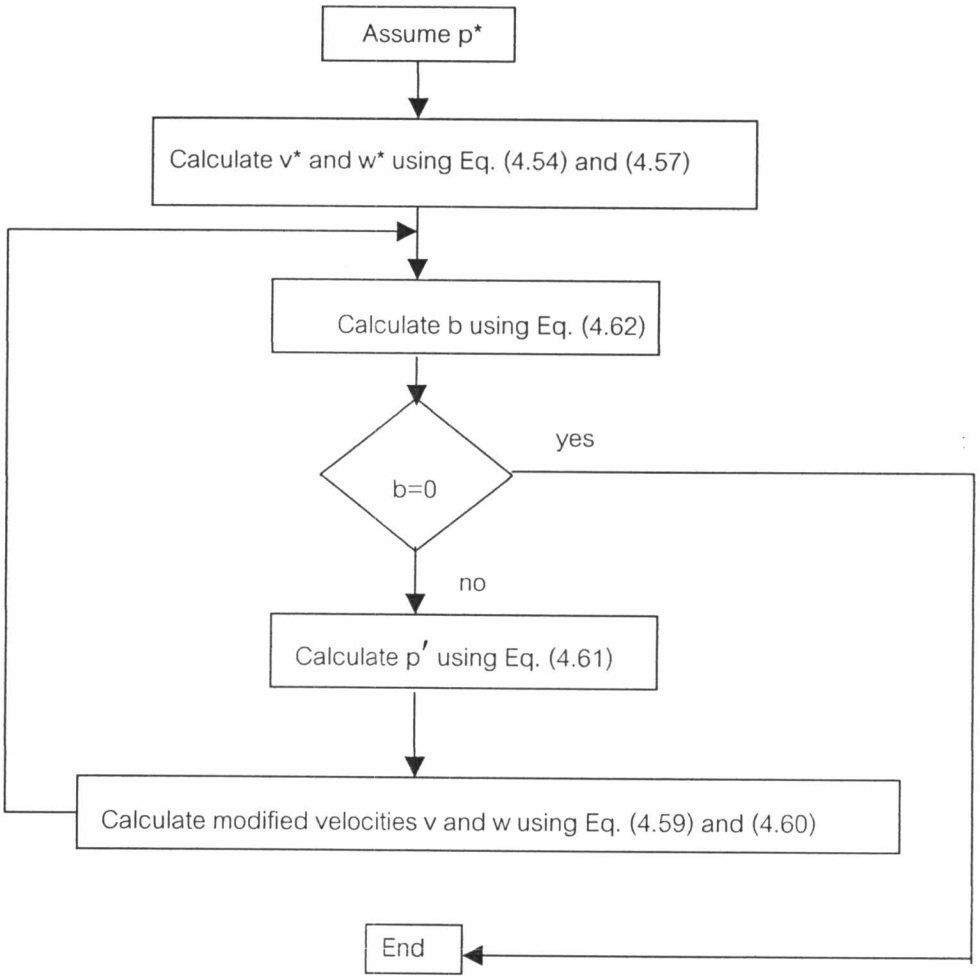

Figure 4.9 Algorithm of modify pressure and velocity

4.3.3 The SIMPLE method

The procedure that we are developing for the calculation of the flow field has been the name SIMPLE, which stands for Semi-Implicit Method for Pressure-Linked Equations. The procedure has been described in Patankar and Spalding (1972) and Patankar (1975).

4.3.3.1 Sequence of operations

1) Guess the pressure field p^*.
2) Solve the momentum equations, such as Equations.(4.54) and (4.57) to obtain v^*, w^*
3) Solve the p' equation from Equation (4.61)
4) Calculate p from $p = p^* + p'$ by adding p' to p^*
5) Calculate v, w from their starred values using the velocity-correction formulas Equations (4.59) and (4.60).
6) Solve the discretization equation for other ϕs (such as temperature, concentration, and turbulence quantities) if they influence the flow field through fluid properties, source terms, etc. (if a particular ϕ does not influence the flow field, it is better to calculate it after a converged solution for the flow field has been obtained.)
7) Treat the corrected pressure p as a new guessed pressure p^*, return to step 2, and repeat the whole procedure until a converged solution is obtained.

The algorithm of the SIMPLE method is shown in Figure 4.10.

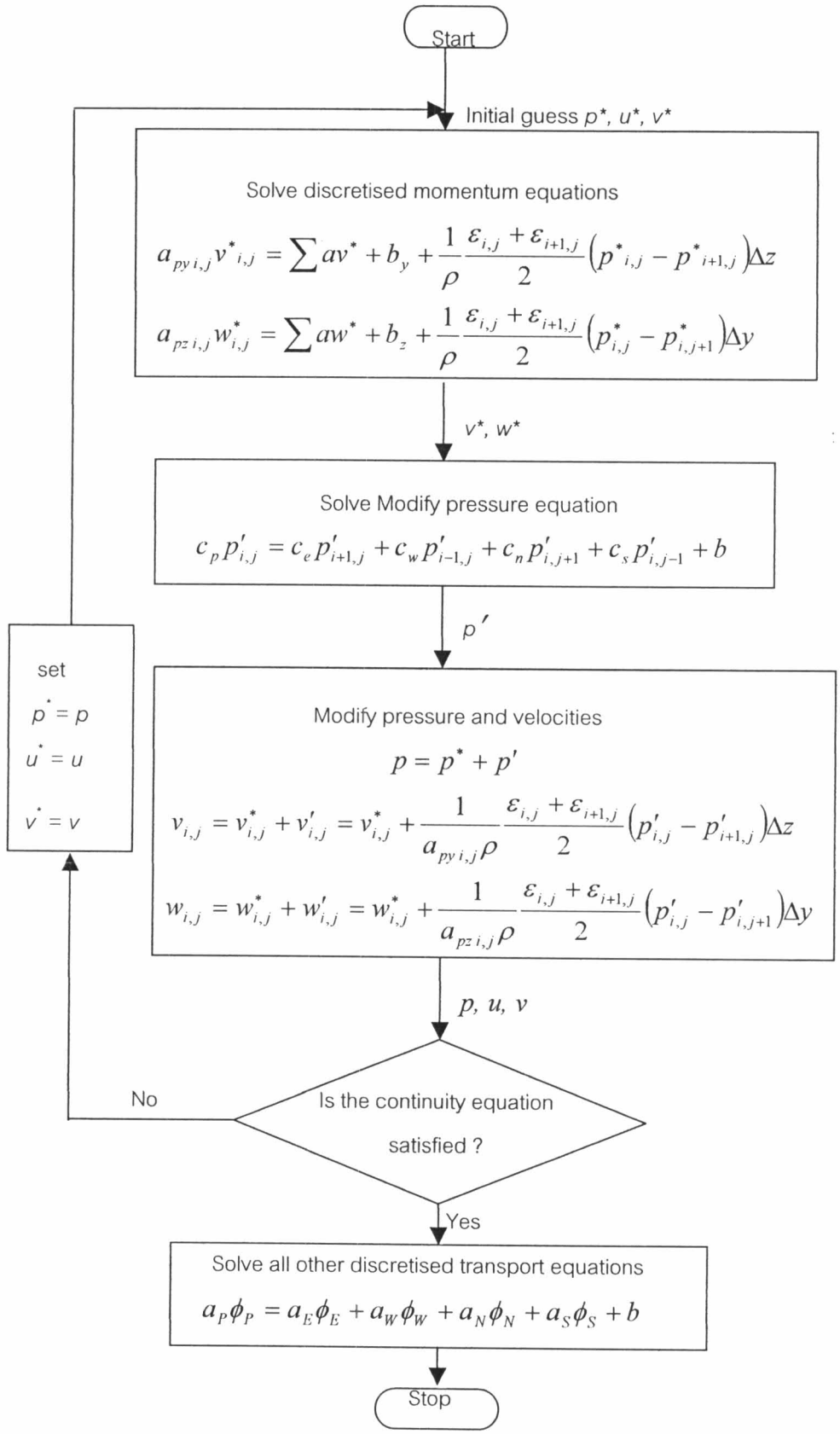

Figure 4.10 The algorithm of the SIMPLE method